

2007

Detailed Mechanistic and Optimization of the Photochemical Production Method of Superoxide

Ta-Chung Ong
Colby College

Follow this and additional works at: <http://digitalcommons.colby.edu/honorstheses>

 Part of the [Chemistry Commons](#)

Colby College theses are protected by copyright. They may be viewed or downloaded from this site for the purposes of research and scholarship. Reproduction or distribution for commercial purposes is prohibited without written permission of the author.

Recommended Citation

Ong, Ta-Chung, "Detailed Mechanistic and Optimization of the Photochemical Production Method of Superoxide" (2007). *Honors Theses*. Paper 267.

<http://digitalcommons.colby.edu/honorstheses/267>

This Honors Thesis (Open Access) is brought to you for free and open access by the Student Research at Digital Commons @ Colby. It has been accepted for inclusion in Honors Theses by an authorized administrator of Digital Commons @ Colby. For more information, please contact enrhodes@colby.edu.

Detailed mechanistic and optimization of the photochemical
production method of superoxide

By Ta-Chung Ong

A Thesis Presented to the Department of Chemistry,
Colby College, Waterville, ME
In Partial Fulfillment of the Requirements for Graduation
With Honors in Chemistry

Submitted May 21, 2007

Detailed mechanistic and optimization of the photochemical
production method of superoxide

By Ta-Chung Ong

Approved:

(Mentor. D. Whitney King, Miselis Professor of Chemistry)

_____ Date

(Reader. Thomas W. Shattuck, Professor of Chemistry)

_____ Date

Vitae

Ta-Chung Ong

Born April 7, 1985

Taipei, Taiwan

Diploma 2003

Pullman High School

Pullman, Washington

Bachelor of Arts 2007

Physics/Chemistry

Colby College

Waterville, Maine

Acknowledgement

This research is supported by a grant from the National Science Foundation obtained by Professor D. Whitney King.

I would like to thank Nathan Boland for much of the previous work of this project, Ali Fulreader for the work on hydrogen peroxide assay, and Professor Dasan Thamattoor for help with the LFP.

I would also like to thank Lauren Brown, Katie Harris, Erin Bast and Andrew Young for being tolerant lab partners.

Many thanks to Hengtian Lin and Ding Ma for being great friends during my four years of college.

Lots of thanks to my family for funding and supporting my education thousands of miles from home. Thanks to Ralph J. Bunche Scholarship and Dana Scholarship for their support. Thanks to Sandra Sohne-Johnson and Michael Walsh for introducing me and my family to Colby College.

Finally, my biggest gratitude to Professor King and family for their guidance and hospitality during this project. This project could not be finished without their support.

Table of Contents

List of Figures	6
List of Tables	7
Abstract	8
Introduction	9
Methods and Materials	17
Results and Discussions	20
Conclusion	41
Future Work	41
Work Cited	42
Appendix A – LFP STELLA Model.....	43
Appendix B – The Continuous Photolysis STELLA Model.....	45

List of Figures

Figure 1: The pH dependence of the observed disproportionation rate constant (k_{obs}) of O_2^- to .. O_2 and H_2O_2	13
Figure 2: Production of O_2^- through photolysis.....	15
Figure 3: Superoxide Production Setup	18
Figure 4: Superoxide absorbance as a function of time in the photolysis experiment	21
Figure 5: Effective extinction coefficients of superoxide and hydrogen peroxide as a function .. of pH	22
Figure 6: Fit of Juice absorbance as a function of time	24
Figure 7: Sample residual plot of experimental absorbance data to the Excel model of the	26
Figure 8: Hydrogen peroxide concentration calculated by the model compared to the	27
concentration measured by the assay at various pH	
Figure 9: Calculated k_{obs} of superoxide disporportionation from experimental data compared .. to to the theoretical k_{obs}	28
Figure 10: Decay of benzophenone triplet and benzophenone ketyl radical intermediates.....	30
Figure 11: Concentraion of superoxide and benzophenone triplet in the LFP STELLA model...	33
Figure 12: Superoxide percentage yield as a function of EtOH concentration	35
Figure 13: STELLA simulation of the production of superoxide at various alcohol	36
concentrations at pH 13.5	
Figure 14: STELLA simulation of the production of superoxide at various pH in 3 M EtOH ...	37
Figure 15: Superoxide concentration produced as a function of pH at 3 M EtOH	39
Figure 16: Superoxide concentration as a function of ethanol concentration at pH 13	40
Figure A1: The LFP STELLA model.....	43
Figure B1: The continuous photolysis STELLA model.....	45

List of Tables

Table I: Reaction Rate Constants of Superoxide disproportionation and various benzophenone triplet reactions	11
Table II: Extinction coefficient of superoxide and hydrogen peroxide species	22
Table III: Literature and experimental values of the decay rate constants of benzophenone diradical (triplet) and benzophenone ketyl radical in the superoxide photochemical production reaction	31

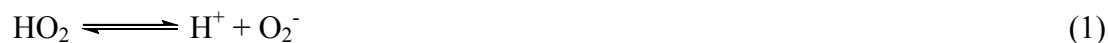
Abstract

The highly reactive nature of superoxide anion presents an analytical challenge to prepare stable standards for instrument calibration. McDowell et al. (1983) developed a convenient method of superoxide production based on continuous photolysis of benzophenone and acetone in oxygen saturated, alkaline, 2-propanol solution. In the McDowell reaction, ketones are photolyzed to their triplet state, and then reacted with alcohol to produce ketyl radicals that react with oxygen to produce superoxide. This study investigated the mechanism and rate of these reactions by Laser Flash Photolysis (LFP). Reaction rate constants for the reaction between the benzophenone triplet and ethanol was $5.5 \times 10^5 \text{ M}^{-1}\text{s}^{-1}$, and between the benzophenone ketyl radical and oxygen was $1.8 \times 10^9 \text{ M}^{-1}\text{s}^{-1}$, consistent with published literature values. The reaction rates and mechanism were incorporated into a STELLA-based kinetic model to predict superoxide production and decay on a time scale of minutes. The model provided optimal conditions for superoxide production in terms of pH and alcohol concentration. The model predictions of superoxide production agree with experimental photolysis results. The model shows that the optimal condition of superoxide production is at 12 M alcohol concentration (ethanol) at pH 13. The actual photolysis results show that the optimal alcohol concentration is 6-9 M at pH 13.

Introduction

Superoxide (O_2^-) is a paramagnetic free radical formed by the one electron reduction of oxygen (O_2). This reaction occurs photochemically in the surface water of lakes or the oceans, in living organisms as a byproduct of mitochondrial respiration, or abiotically as a result of trace metal redox recycling. In the cell, superoxide is toxic because of its ability to oxidize and reduce metal ions attached to biological targets, thereby degrading the target through electron transfer reactions.¹ Organisms counter superoxide with the enzyme superoxide dismutase (SOD), which can have manganese, zinc, or copper/zinc as cofactors. In aqueous media, superoxide takes part in the redox cycling of dissolved trace metal ions such as iron and copper just like in biological systems, and as a result produces hydrogen peroxide, another reactive oxygen species. This property makes the study of superoxide of interest in environmental biology and chemistry because iron is a cofactor for metabolic activity such as photosynthesis, and therefore essential for marine microorganism growth.² It was observed that marine phytoplankton produce superoxide at the cell surface, allowing organisms to reduce and uptake iron at the cell surface to meet physiological metal requirements.³ The focus of this paper is on photochemical production of superoxide in aqueous media.

Superoxide exists either as the weak acid (HO_2) or the conjugate base (O_2^-) with the fraction of each determined by solution pH. The acid dissociation reaction of superoxide is



with a dissociation constant of $-\log K = 4.5$ (K listed in Table I). Most analytical measurements of superoxide measure the protonated and unprotonated form of superoxide because the proton transfer reaction is fast relative to the analytical method. The total superoxide concentration, $T_{O_2^-}$, is calculated from the mass balance of HO_2 and O_2^- ,

$$T_{O_2^-} = [HO_2] + [O_2^-] \quad (2).$$

The fraction of each superoxide species may be computed,

$$\alpha_0 = \frac{[HO_2]}{[T_{O_2^-}]} = \frac{[HO_2]}{[HO_2] + [O_2^-]} = \frac{H^+}{K_1 + H^+} \quad (3)$$

$$\alpha_1 = \frac{[O_2^-]}{[T_{O_2^-}]} = \frac{[O_2^-]}{[HO_2] + [O_2^-]} = \frac{K_1}{K_1 + H^+} \quad (4)$$

and so the concentration of superoxide,

$$[HO_2] = \alpha_0 [T_{O_2^-}] \quad (5)$$

$$[O_2^-] = \alpha_1 [T_{O_2^-}] \quad (6)$$

Superoxide decays through a disproportionation reaction to hydrogen peroxide and oxygen.



The rate laws of reactions (7) and (8) are

$$-\frac{d[HO_2]}{dt} = k_7 [HO_2]^2 \quad (10)$$

$$-\frac{d[O_2^-]}{dt} = k_8 [HO_2][O_2^-] \quad (11)$$

with the overall superoxide disproportionation rate the sum of rate (10) and rate (11)

$$-\frac{d[T_{O_2^-}]}{dt} = k_7 [HO_2]^2 + k_8 [HO_2][O_2^-] \quad (12)$$

Eq. (12) shows that the protonated state of superoxide has a significant influence on overall reaction rate.

Table I. Reaction Rate Constants of Superoxide disproportionation and various benzophenone triplet reactions

Reaction	Reaction Equation	Rate Constant ($M^{-1}s^{-1}$)	Reference
1	$HO_2 \rightleftharpoons H^+ + O_2^-$	1.60×10^{-5} (M) (Dissociation K)	4
7	$HO_2 + HO_2 \rightarrow H_2O_2 + O_2$	8.30×10^5	4
8	$HO_2 + O_2^- \rightarrow HO_2^- + O_2$	9.70×10^7	4
17	${}^3Ph_2CO \rightarrow Ph_2CO$	$6.73 \times 10^5 s^{-1}$	8
18	${}^3Ph_2CO \xrightarrow{O_2} Ph_2CO$	2.6×10^9	8
19	${}^3Ph_2CO + (CH_3)_2CHOH \rightarrow$ $Ph_2\dot{C}OH + (CH_3)_2\dot{C}OH$	2.1×10^6	7
21	$Ph_2\dot{C}OH + O_2 \rightarrow O_2^- + Ph_2CO$	2.3×10^9	8

Since the concentration of the protonated and unprotonated superoxide is given by Eq. (3) and (4), they can be substituted into Eq. (12), to define the rate equation for superoxide in terms of total, analytical, concentrations.

$$-\frac{d[T_{O_2^-}]}{dt} = (k_7\alpha_0\alpha_0 + k_8\alpha_0\alpha_1)[T_{O_2^-}]^2 \quad (13)$$

Therefore, the observed rate of superoxide disproportionation is a second order reaction

$$-\frac{d[T_{O_2^-}]}{dt} = k_{obs}[T_{O_2^-}]^2 \quad (14)$$

with the observed rate constant, k_{obs}

$$k_{obs} = k_7\alpha_0\alpha_0 + k_8\alpha_1\alpha_0 \quad (15)$$

Substituting Eq. (3) and Eq. (4), k_{obs} becomes

$$k_{obs} = k_7 \frac{[H^+]^2}{(K_a + H^+)^2} + k_8 \frac{[H^+][K_a]}{(K_a + H^+)^2} \quad (15-b)$$

The observed second-order reaction is dependent on the magnitude of α_0 and α_1 , and thus pH dependent as shown in Eq. (15-b) and Fig. 1. At lower pH, the HO_2/HO_2 reaction dominates, and the rate constant is pH independent. At the pKa of superoxide, where α_0 equals α_1 , k_{obs} is at its maximum. Past the pKa, the HO_2/O_2^- reaction dominates, and k_{obs} reduces by one order of magnitude for every unit increase of pH.⁴

As a second order reaction, superoxide has a half life given by

$$\tau_{1/2} = \frac{1}{k_{obs}[T_{O_2^-}]} \quad (16)$$

In natural waters with a pH of 7, $k_{obs} \approx 5 \times 10^5 \text{ M}^{-1} \text{ s}^{-1}$ and superoxide at μmolar concentrations, the half life of superoxide is 2 sec. This short half life makes analytical measurements and the study of superoxide difficult because superoxide standards are not stable. To counter this instability, the study of superoxide needs to be done in an alkaline solution in laboratory setting, taking advantage

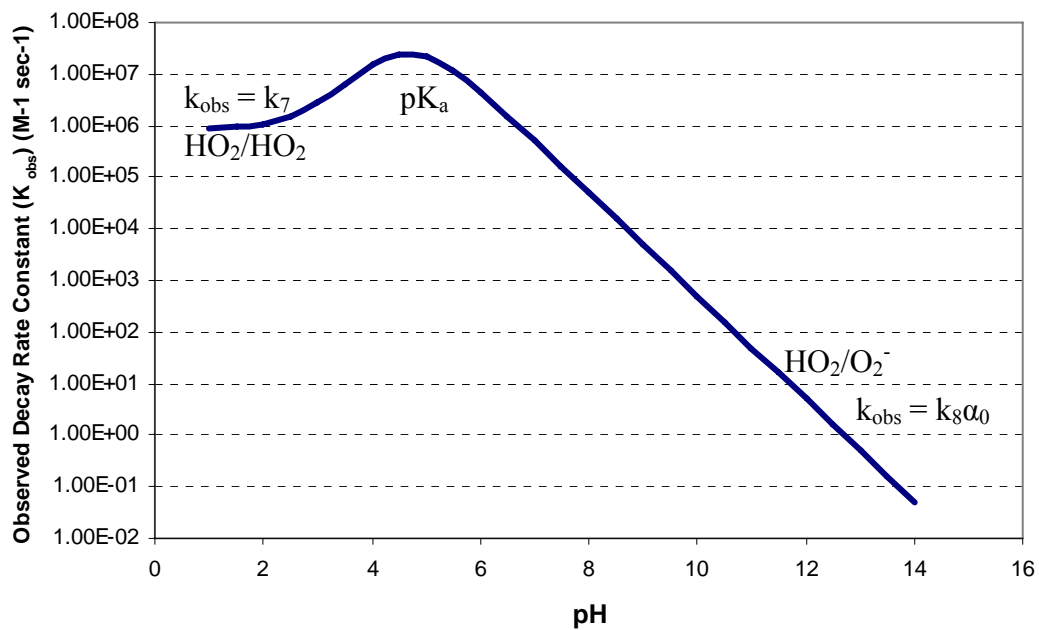


Fig. 1. The pH dependence of the observed disproportionation rate constant (k_{obs}) of O_2^- to O_2 and H_2O_2 . The decay rate constant reaches maximum at the pK_a of superoxide dissociation reaction. As pH approaches zero, the reaction rate constant approaches k_2 as $[\text{O}_2^-]$ becomes negligible and the HO_2/HO_2 reaction dominates. As pH increases past the pK_1 , the HO_2/O_2^- reaction dominates, the rate constant decreases by one order of magnitude per unit increase in pH (adapted from ref. 4).

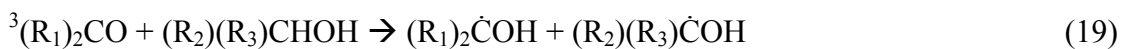
of the fact that k_{obs} is smaller in basic condition as shown in Fig. 1. Unfortunately, commercially available superoxide salts are notoriously dirty and not suitable for careful analytical work.

Therefore, an alternative source of superoxide is needed. McDowell et al. (1983) devised a simple technique for superoxide production based on photolysis of substituted ketones in oxygen-saturated, alkaline, 2-propanol solution, shown in Fig. 2.⁵ Fujii et al. (2006) used ethanol, instead of 2-propanol, and at higher alcohol concentration than McDowell to optimize the reaction.⁶ The work of these authors gives a clean source of superoxide.

However, these previous works did not include detailed mechanistic information for the superoxide production reaction. It is our interest to study the reaction's detailed mechanism to optimize conditions for superoxide production, and test the validity of using single absorbance measurements to quantify superoxide production. We are interested in investigating the rates of reaction of each individual reaction step shown in Fig. 2, and modeling the results in the context of McDowell's reaction. LFP was used to measure concentration of radical intermediates and observe their decay over short period of time in nanosecond and microsecond range, and steady state photolysis was used to implement this chemistry in a bench scale reactor.

Mechanism

The photolysis of ketones with UV light produces an excited state triplet radical with high quantum efficiency.⁹ The triplets undergo three reactions including non-radiative relaxation back to the ground state, quenching by O_2 , or reaction with alcohol to produce ketyl radical.



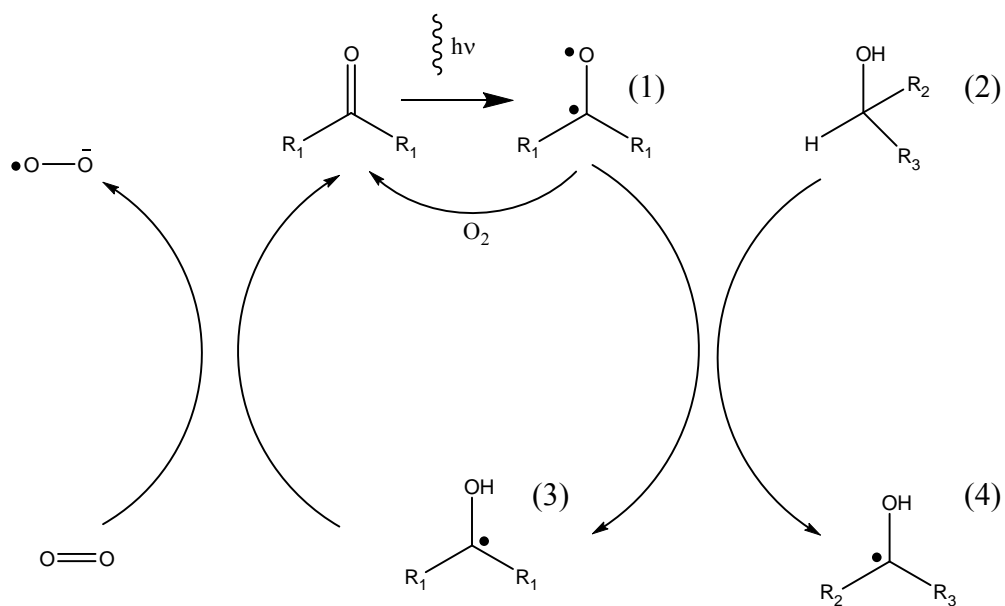


Fig. 2. Production of O_2^- through photolysis. The ketone is photolyzed, producing a ketone triplet, (1). (1) then reacts with an alcohol, (2), to produce two carbon centered radicals, (3) and (4), or returns to the ground state. Both (3) and (4) can react with oxygen gas to produce O_2^- as well as returning the ketone, allowing the cycle to continue. (In McDowell, R_1 is a phenyl group, R_2 and R_3 are methyl groups) (In Fujii, R_1 and R_2 are methyl groups, and R_3 is a hydrogen) (adapted from ref. 5)

Reaction (17) shows the non-radiative relaxation of the ketone triplet back to benzophenone singlet. Reaction (18) shows the quenching of triplet by oxygen. Reaction (19) shows the production of ketyl radicals by reaction of ketone triplet with alcohol, which is the same reactions as shown in Fig. 2. These processes have been well studied for benzophenone by Shield et al. (1998) using time-resolved fluorescence and by Canonica et al. (2000) using laser flash photolysis.^{7,8}

The produced ketyl radical is a weak acid and undergoes dissociation:



With the pKa is 9.2 for benzophenone ketyl radical.⁹ Both protonated and deprotonated ketyl radicals may react with oxygen to produce superoxide and ketone, reforming the original chromophore:⁸



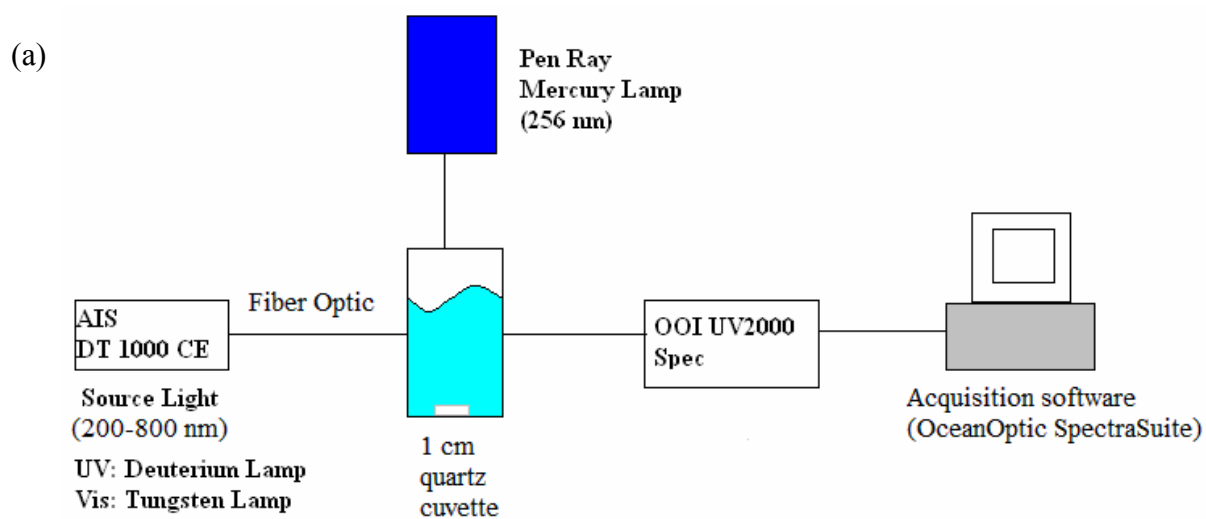
There are three parts to this work. The first part is the investigation of the superoxide production in continuous photolysis, using acetone and ethanol. The second part is the investigation of fast kinetics in intermediate steps using laser flash photolysis, with benzophenone replacing acetone as a more suitable chromophore at the laser wavelength. The substitution is necessary because acetone does not absorb well in the 355 nm Nd-YAG laser wavelength. By substituting acetone with benzophenone, an assumption is made that the intermediates of both species would react with similar mechanistic information. This assumption is largely based on the structural similarity between acetone and benzophenone, which is that both molecules have the form $(R_1)_2CO$. The third part is the computer modeling of continuous photolysis using data from the fast kinetic study, which informs further continuous photolysis experiments.

Methods and Materials

Material. All solutions were made using 18 M Ω Milli-Q water. Ethanol (absolute, 99.5%, ACS) and sodium hydroxide (pellets) were purchased from Acros. Acetone (spectranalyzed), benzophenone, and boric acid were from Fisher. Diethylenetriaminepentaacetic acid (DTPA) anhydride was from Sigma. All reagents were used without further purification.

Superoxide stock solution production. Superoxide is produced via photolysis of acetone and alcohol solution via modified methods first proposed by McDowell and Fujii.^{5,6} The instrument, also called the “Juicer”, consists of two parts, the photolysis setup for the generation superoxide, and the detection setup for the detection of superoxide. The photo and schematic of the instrument are shown in Fig. 3. In the photolysis setup, an excitation source illuminates a quartz cuvette containing the acetone and alcohol solution to generate superoxide. To keep the cuvette temperature constant during the photolysis, the cuvette is cooled in a metal holder with flowing water during the experiment, and stirred with a magnetic stir bar. The excitation source is a Pen Ray mercury lamp (Model PS-1, 115 V, 60 Hz, 0.40 Amps, 10 W). The detection setup is a fiber optic UV/Vis spectrophotometer employing an AIS deuterium/tungsten lamp (Model DT 1000 CE), and a charged coupled device detector, Ocean Optics Inc. UV2000 (OOI UV2000) Spec. The acquisition speed was 100 ms and each acquisition included the entire spectrum from 200 to 800 nm. Absorbance at 240 nm was measured as the superoxide absorbance, after subtraction of the absorbance at 400 nm to account for background.

The acetone and alcohol solution, also called The “Juice”, consists of 41 mM of acetone, 3-12 M of ethanol, and 30 μ M of DTPA in 1 mM boric acid buffer of various pH from 11 to 13 adjusted using sodium hydroxide. The solution is saturated with pure oxygen, then photolyzed by the mercury lamp for 30-60 seconds to a desired superoxide concentration. Benzophenone was tried at 6.3 μ M as a substitute to acetone, but acetone was favored due to better solubility in aqueous



(b)

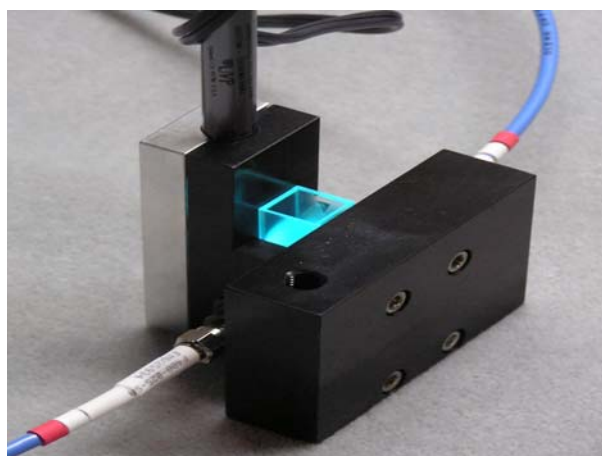


Fig. 3. (a) Superoxide Production Setup (The “Juicer”). The acetone and alcohol solution (“Juice”) is photolyzed by the Mercury Lamp in 1 cm quartz cuvette. The deuterium source light illuminates the cuvette 90° from the Mercury Lamp. Signals received by the charged couple detectors (OOI UV 2000 Spec.) are sent to a computer with acquisition software, which integrate and average the signals. To keep the cuvette temperature constant, it is cooled by a metal holder with flowing water during the experiment (not shown). (b) A picture of the instrument during photolysis, showing the mercury lamp and the cuvette. The two cords are fiber optics, one connects the cuvette to the source light, the other to the OOI UV 2000 Spec. detector.

solution. Isopropanol was tried at the same concentration as ethanol, but ethanol was favored because ethanol radical reaction with oxygen would not generate additional acetone.

Laser Flash Photolysis (LFP). LFP was performed using a Luzchem LFP employing a Quantel Nd-YAG pulse laser as the excitation source. The laser was wavelength tripled to 355 nm by second harmonic generation with potassium hydrogen phosphate. The source light of the Luzchem LFP is a Xe lamp, and the detector is a fast PMT connected to a 2 GHz digital oscilloscope and data logger. Each pulse laser delivered 40 mJ of power with pulse width of 10 ns. The temporal resolution of laser flash photolysis experiments were 10 nsec to milliseconds.

Since acetone radical intermediates do not absorb well in the 355 nm laser wavelength, benzophenone is used instead as a molecular analog to acetone. The solution for LFP uses 2.5 mM benzophenone diluted in different concentrations of ethanol (50% to 80%) and 1 mM borax buffer with pH ranging from acidic to basic. The benzophenone ketyl radical absorbance in the basic condition was measured at 635 nm, and in acidic conditions was measured at 535 nm. Absorbance at 530 nm is measured as the benzophenone diradical absorbance. The decay time-trace obtained was fit as a first-order or second-order decay using the instrument's software.

Results and Discussions

Quantification of superoxide. A typical photolysis run is shown in Fig. 4. The mercury lamp is turned on at $t = 4$ sec, and turned off at $t = 64$ sec, resulting in an increase of absorbance at 240 nm due to the accumulation of superoxide. After $t = 64$ sec the absorbance decreases as superoxide disproportionates to hydrogen peroxide, which has a smaller extinction coefficient.

The absorbance measurement is described by Beer's Law:

$$A = \epsilon bc \quad (23)$$

Where A is the measured absorbance, ϵ is the extinction coefficient, b is source light's path length, and c is concentration. At 240 nm, both superoxide and hydrogen peroxide absorb, and so the total absorbance is the sum of the absorbance of each species

$$A = b(\epsilon_{O_2^-}^* [T_{O_2^-}] + \epsilon_{H_2O_2}^* [H_2O_2]) \quad (24)$$

where ϵ^* are the effective extinction coefficients for superoxide and hydrogen peroxide at 240 nm.

The effective superoxide and hydrogen peroxide extinction coefficient are calculated based on their weak acid properties, where ϵ^* is the speciation weighted average of the acid and basic forms of each chromophore.⁴

$$\epsilon_{O_2^-}^* = \frac{[HO_2]}{[HO_2] + [O_2^-]} \epsilon_{HO_2} + \frac{[O_2^-]}{[HO_2] + [O_2^-]} \epsilon_{O_2^-} \quad (25)$$

By substituting Eq. (3) and (4), Eq. (23) becomes

$$\epsilon_{O_2^-}^* = \frac{[H^+]}{(K_\alpha^{HO_2} + [H^+])} \epsilon_{HO_2} + \frac{K_\alpha^{HO_2}}{(K_\alpha^{HO_2} + [H^+])} \epsilon_{O_2^-} \quad (25-b)$$

Similarly,

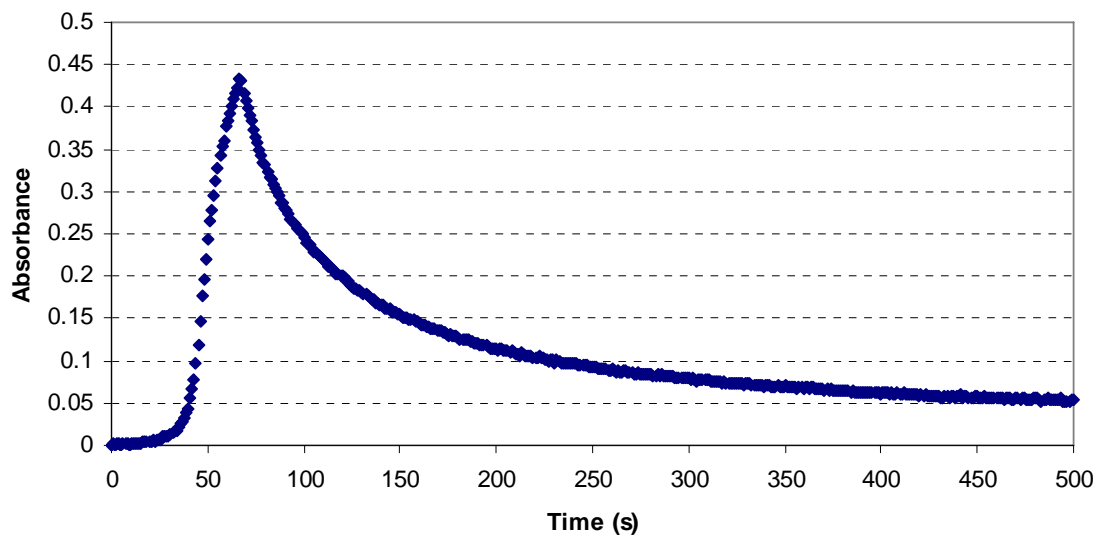


Fig. 4. Superoxide absorbance as a function of time in the photolysis experiment. The mercury lamp was turned on at $t = 4$ sec, and off at $t = 64$ sec. In this time frame, absorbance increases as superoxide accumulates. After $t = 64$ sec, absorbance decreases as superoxide decays to hydrogen peroxide, which has a smaller extinction coefficient.

Table II. Extinction coefficient of superoxide and hydrogen peroxide species⁴

Species	ϵ 240 nm
HO_2	1260
O_2^-	2345
H_2O_2	31
HO_2^-	320

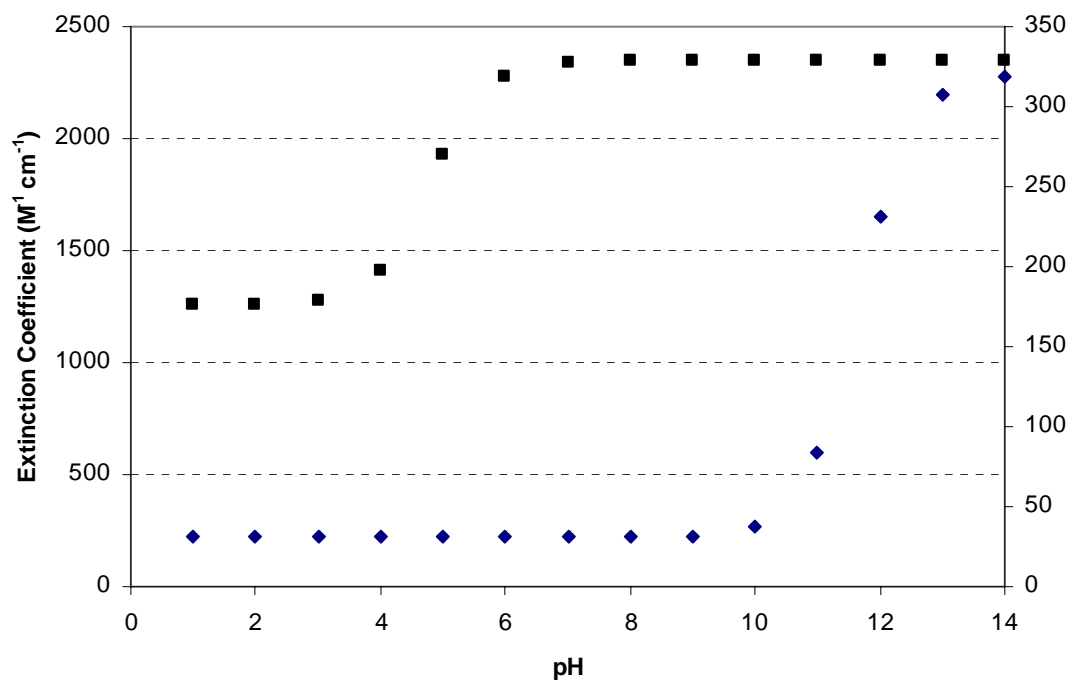


Fig. 5. Effective extinction coefficients of superoxide and hydrogen peroxide as a function of pH. The squares (■) are extinction coefficients of superoxide at various pH with magnitude shown at the left-handed y-axis. The diamonds (◆) are extinction coefficients of hydrogen peroxide, with magnitude shown at the right-handed y-axis.

$$\varepsilon_{H_2O_2}^* = \frac{[H^+]}{(K_\alpha^{HOOH} + [H^+])} \varepsilon_{H_2O_2} + \frac{K_\alpha^{HOOH}}{(K_\alpha^{HOOH} + [H^+])} \varepsilon_{HO_2^-} \quad (26)$$

The effective extinction coefficients are thus functions of pH as shown in Fig. 5, the extinction coefficient of each species is listed in Table II.

To model the decay of superoxide, the absorbance of superoxide is collected over time and fit to a second order rate law

$$\frac{d[O_2^-]}{dt} = k_{obs} [T_{O_2^-}]^2 \quad (27)$$

The superoxide concentration at the beginning of the decay is given by the concentration at the end of photolysis,

$$[O_2^-]_0 = \frac{(A_0 - \varepsilon_{HOOH}^* b[H_2O_2]_0)}{b\varepsilon_{O_2^-}^*} \quad (28)$$

where A_0 is the measured absorbance at the end of photolysis, corrected to account for absorbance due to hydrogen peroxide. The concentration of superoxide as a function of decay time is given by the simple second order integrated rate law

$$[O_2^-]_t = \frac{1}{\left(\frac{1}{[O_2^-]_0} + k_{obs}t\right)} \quad (29)$$

The concentration of hydrogen peroxide as a function of time is given by

$$[H_2O_2]_t = [H_2O_2]_0 + \frac{1}{2}([O_2^-]_0 - [O_2^-]_t) \quad (30)$$

which follows from the stoichiometry of superoxide disproportionation from Eq. (7) and (8). The absorbance at 240 nm calculated using Excel at any given time is

$$A_t = \varepsilon_{O_2^-}^* b[O_2^-]_t + \varepsilon_{H_2O_2}^* b[H_2O_2]_t \quad (31)$$

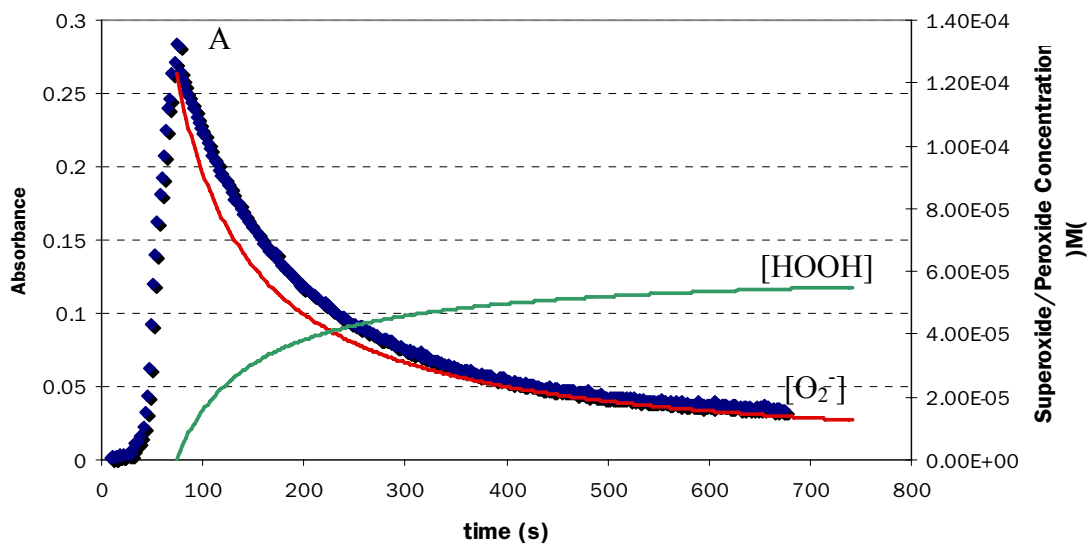


Fig. 6. Fit of Juice absorbance as a function of time. Absorbance is collected over a period of time, showing both the superoxide production from photolysis (increase in absorbance) and decay after photolysis (decrease in absorbance). Excel non-linear fitting is used to calculate the concentration of superoxide as it decays and hydrogen peroxide as it grows over time.

The values of $[\text{H}_2\text{O}_2]_0$ and k_{obs} are calculated using Excel to perform a non-linear fit of the absorbance data to Eq. (31) where $[\text{O}_2^-]_t$ and $[\text{H}_2\text{O}_2]_t$ are defined by Eq. (29) and (30) respectively. A typical fit is shown in Fig. 6.

Fig. 7 is the calculated absorbance using Eq. (31) fit to experimental data. The error in the fit to the absorbance data is less than 5×10^{-3} . This fit shows that the model accurately captures superoxide disproportionation and hydrogen peroxide production. To confirm the model a hydrogen peroxide assay was done at the end of several runs to confirm the calculated concentration of hydrogen peroxide matches the experimental value. The concentration of hydrogen peroxide measured by the assay agrees to within a factor of 2 with the model at the end of the decay run as shown in Fig. 8. Propagating this error in hydrogen peroxide concentration to the corresponding superoxide concentration prediction, this inaccuracy corresponds to up to a 30% error for some of the runs. This error indicates that the model can predict with some accuracy the concentration of superoxide and hydrogen peroxide produced in the experiment. The k_{obs} calculated by the model are larger than the literature values published by Bielski et al. However, alcohol increases the rate of superoxide decay by a factor of 2,⁵ and after adjusting for the effect the alcohol, the corrected k_{obs} fall on the Bielski curve as shown in Fig. 9. Lower pH k_{obs} fit closer to the Bielski curve than higher pH. At pH 13, the k_{obs} are off by an order of magnitude from the Bielski curve, indicating that superoxide may be decaying by other mechanisms such as metal catalysis, at high pH. These findings at pH lower than 13 indicate good agreement between the model and the experiment, allowing calculation of superoxide concentrations from raw absorbance measurement.

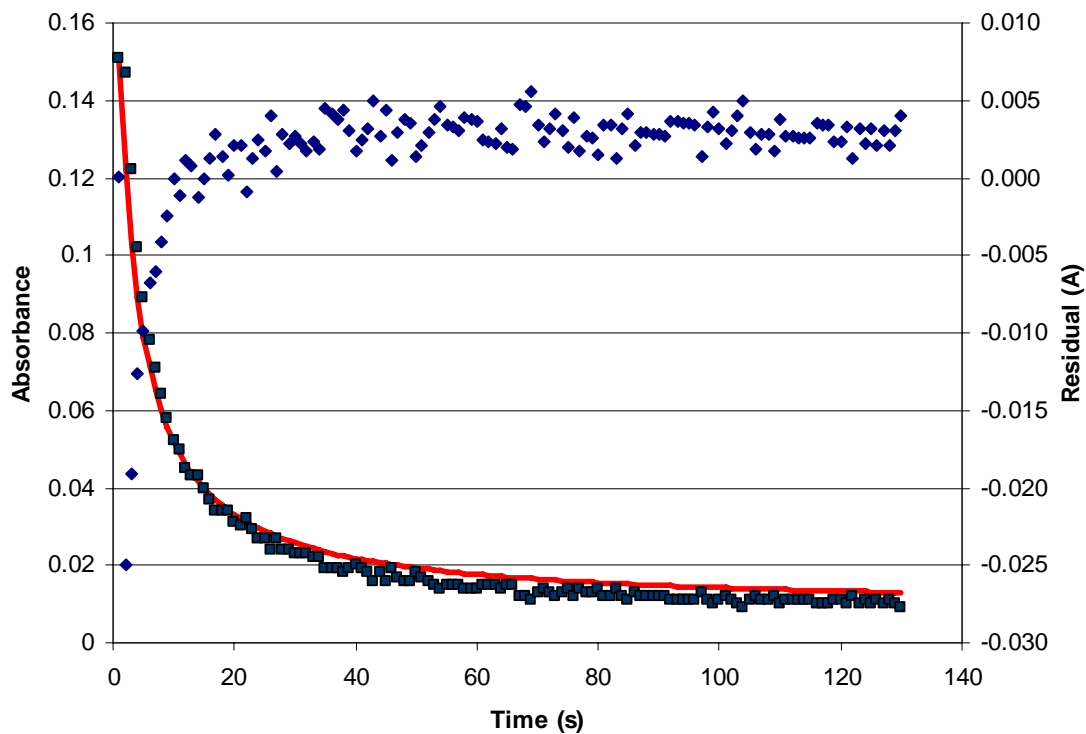


Fig. 7. Sample residual plot of experimental absorbance data to the Excel model of the decay run. The squares (■) are the experimental absorbance data, and the line is the model fit. The diamonds (◆) are the residual absorbance between the experimental and the model values. The magnitude of the residual is less than 5×10^{-3} absorbance unit past the first few seconds of the decay run, indicating good agreement between the model and the experiment. The larger residual at the beginning of the decay is attributed to the mixing in of the small amount of superoxide that is produced past the immediate end of photolysis.

[HOOH] Dependence on pH (3M EtOH Only)

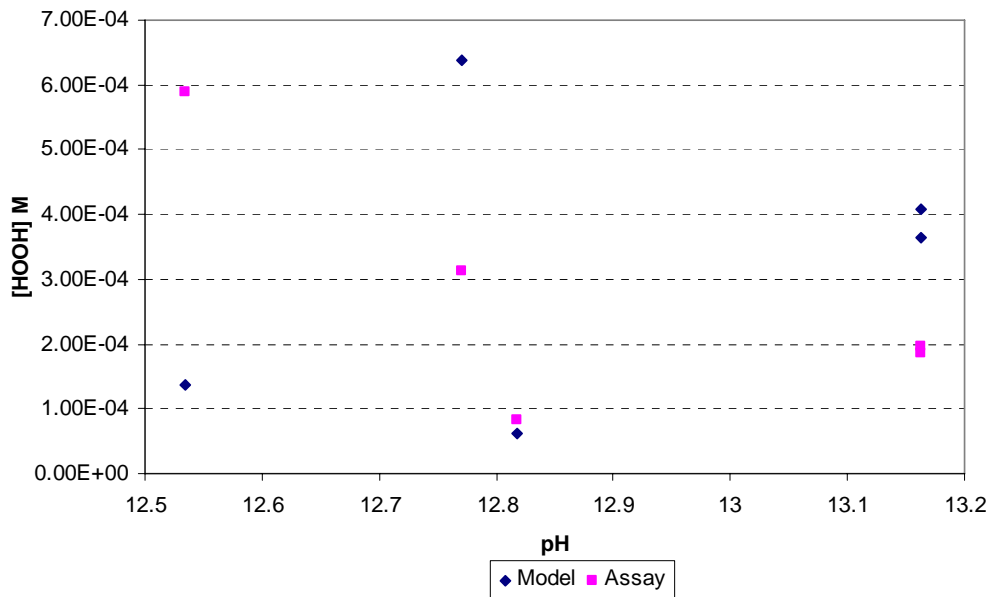


Fig. 8. Hydrogen peroxide concentration calculated by the model compared to the concentration measured by the assay at various pH. The model calculated hydrogen peroxide concentration agrees with the assay to within one order of magnitude. Propagating the error in hydrogen peroxide concentration to the corresponding superoxide concentration found up to 30% error in superoxide prediction.

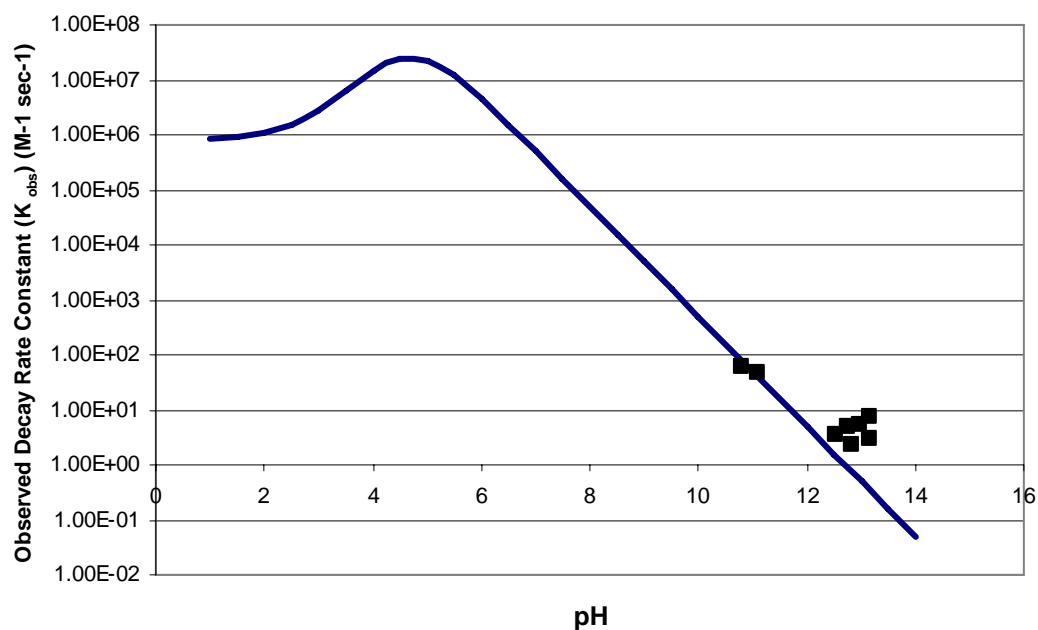


Fig. 9. Calculated k_{obs} of superoxide disproportionation from experimental data compared to the theoretical k_{obs} . The line is the theoretical superoxide disproportionation rate constant as a function of pH published by Bielski et al.⁴ The black squares (■) are k_{obs} calculated by the Excel model using data from the photolysis experiment, corrected for the effect of alcohol. The model calculated k_{obs} fall closely or on the Bielski curve, showing good agreement between the theory and the experiment. The lower pH experiments fit better than the higher pH. At high pH, other reactions such as metal catalysis might become significant in our experiments.

LFP Investigation of Detailed Mechanism. The decay rate constants of the intermediates, benzophenone diradical (triplet) and benzophenone ketyl radical, in the superoxide photochemical production were calculated using a second order fit to the absorbance as a function of time. In high ethanol concentration and oxygen saturated condition, a first order fit was calculated instead since the reaction became pseudo first order due to excess alcohol or oxygen. The pseudo first order decay of benzophenone triplet and benzophenone ketyl radical is shown in Fig. 10. The temporal resolution required to observe benzophenone triplet is on the time scale of 100 ns, while the resolution required to observe benzophenone ketyl radical is on the time scale of microseconds.

The values obtained are compared to the literature values as shown in Table III. We found that the decay rate constant of benzophenone triplet was close to the published values for Reaction (19) at 80% ethanol, indicating that the reaction of the benzophenone triplet with alcohol dominates over relaxation shown by Reaction (17) and (18) at 80% ethanol.

The measured decay rate constant of benzophenone ketyl radical was close to the literature value of Reaction (21), the reaction between the ketyl radical and oxygen. This finding indicates that side reactions such as radical dimerization have minimal impact on the production mechanism under oxygen saturated conditions. In addition, reactivity did not seem heavily influenced by pH as the reaction rate constant of the acidic reaction and basic reaction are within a factor of 2.

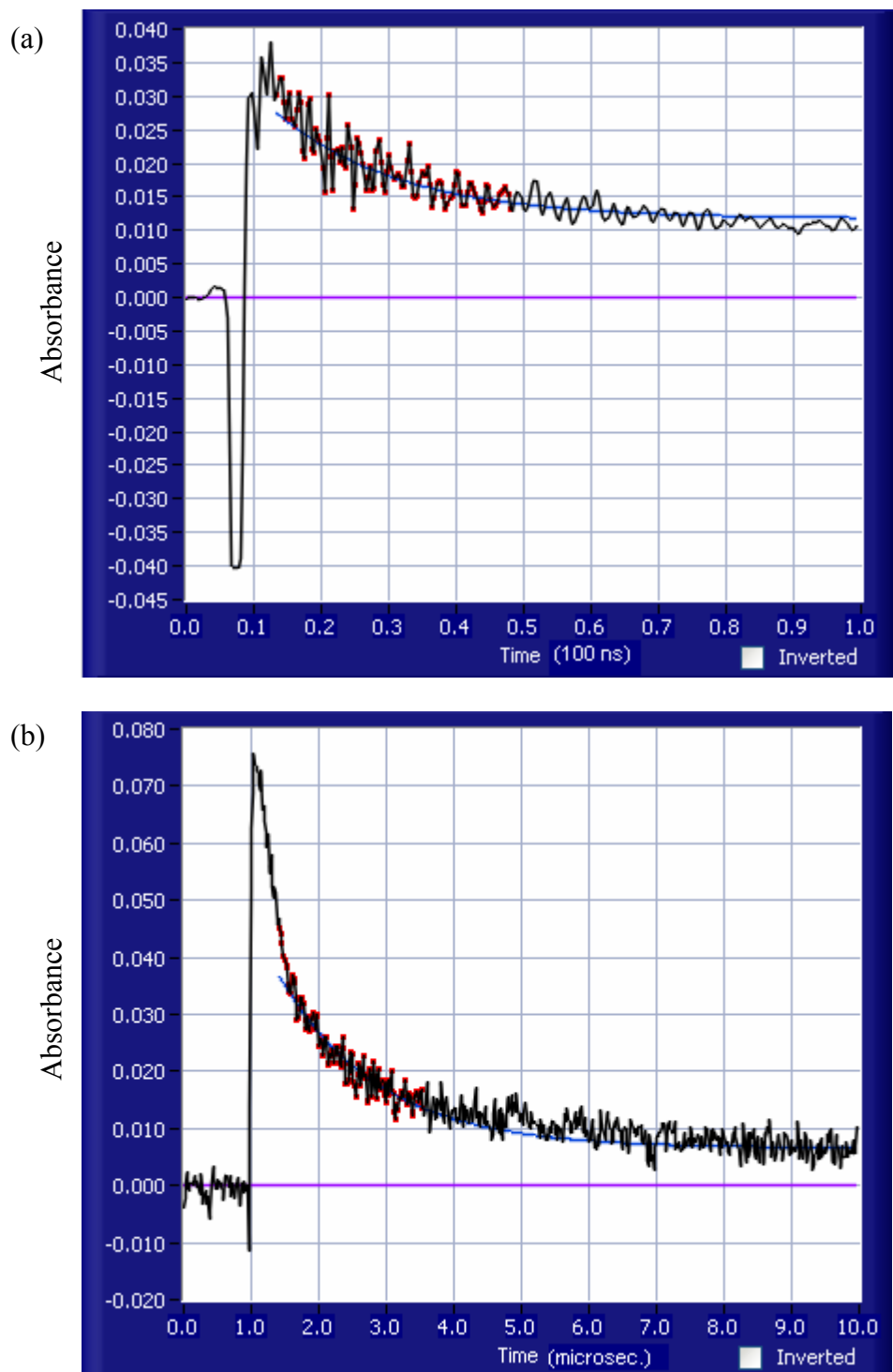


Fig. 10. (a) Pseudo first order decay of benzophenone triplet to benzophenone ketyl radical at 60% ethanol concentration. (b) Pseudo first order decay of benzophenone ketyl radical at oxygenated condition. Temporal resolution required to observe benzophenone triplet is on 100 ns time scale, while the resolution required to observe benzophenone ketyl radical is on microsec time scale.

Table III. Literature and experimental values of the decay rate constants of benzophenone diradical (triplet) and benzophenone ketyl radical in the superoxide photochemical production reaction.

Reaction	Reaction Equation	Rate Constant (M ⁻¹ s ⁻¹) (Literature)	Rate Constant (s ⁻¹) (Literature)	Rate Constant (s ⁻¹) (Experimental) (pH 4.78)	Rate Constant (s ⁻¹) (Experimental) (pH 13.1)
19	³ Ph ₂ CO + (CH ₃) ₂ CHOH → Ph ₂ ĊOH + (CH ₃) ₂ ĊOH	2.1x10 ⁶	2.9x10 ⁷ (80% 2-propanol)	7.6x10 ⁶ (80% EtOH)	8.0x10 ⁶ (80% EtOH)
21	Ph ₂ ĊOH + O ₂ → O ₂ ⁻ + Ph ₂ CO	2.3x10 ⁹	2.3x10 ⁶ (O ₂ saturated, 1 mM)	1.8x10 ⁶ (O ₂ saturated, 1 mM)	3.0x10 ⁵ (O ₂ saturated, 1 mM)

While we used benzophenone as a better chromophore in the LFP experiments, we used acetone in the continuous photolysis experiments for better solubility in aqueous media. We assume the reaction rate constants would be similar between benzophenone and acetone intermediate radicals due to similarity in their structures. That is, the reaction rate constant of acetone triplet and ethanol reaction would be similar to the reaction rate constant of benzophenone triplet and ethanol, and the reaction rate constant of acetone ketyl radical and oxygen reaction would be similar to the reaction rate constant of benzophenone ketyl radical and oxygen. McDowell et. al. (1983) performed superoxide production experiment using both acetone and benzophenone, and the concentration of superoxide produced are comparable.⁵ This finding suggests that both species must react to alcohol similarly, or else no superoxide would have been produced.

STELLA Computer Model. The detailed mechanistic information on the McDowell reaction was obtained from the LFP experiment, and used in the reaction simulation program, STELLA, to investigate the optimal conditions for superoxide production. The model consists of two parts, the production of superoxide (McDowell reaction) and the superoxide decay to hydrogen peroxide (disproportionation). The goal is to maximize the concentration of superoxide produced in the continuous photolysis experiment.

For production, a model of the LFP experiment was built first to investigate superoxide production on a microsecond time scale (See Appendix A for model details). It was found that that the superoxide concentration reaches steady state in 3 microseconds after all triplets are distributed via Reaction (17), (18), or (19), as shown in Fig. 11. The model makes the assumption that every benzophenone triplet produced must either relax

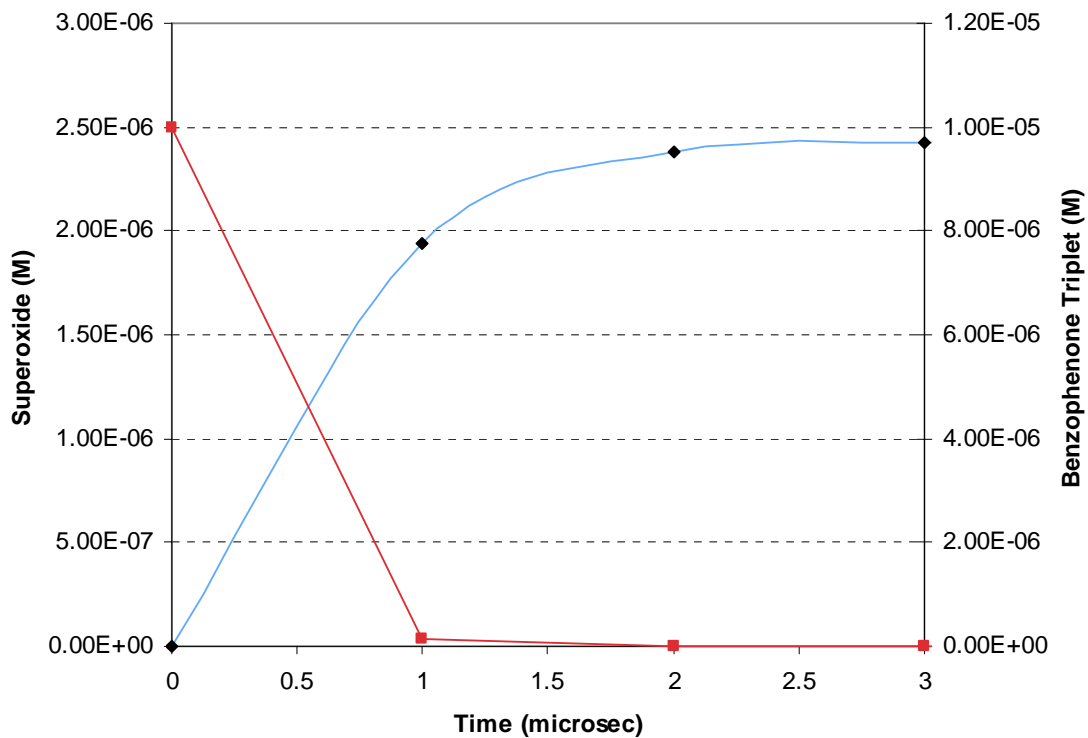


Fig. 11. Concentraion of superoxide and benzophenone triplet in the LFP STELLA model. The diamonds (◆) refer to the superoxide concentration, and the squares (■) refer to the benzophenone triplet concentration. The superoxide concentration reaches steady state in the microsecond time scale once all the benzophenone triplets decay via Reaction (17), (18), or (19).

back to the ground state, or react with alcohol (either 2-propanol or ethanol) to produce superoxide. From this, the efficiency of superoxide production is calculated as:

$$O_2^- \text{ Yield} = \frac{k_{19}[\text{Alcohol}]}{k_{17} + k_{18}[\text{O}_2] + k_{19}[\text{Alcohol}]} \quad (32)$$

where k_{17} and k_{18} refer to the literature value of the reaction rate constant of Reaction (17) and (18) (k_{17} is first-order, k_{18} is second-order), and k_{19} refers to the experimental second-order reaction rate constant of Reaction (19) calculated from the LFP result using EtOH. $[\text{O}_2]$ is set at 1 mM, the oxygen saturated condition, assuming the changes in oxygen solubility at various ethanol concentration would not significantly alter the superoxide production yield. The percentage yield of superoxide increases as a function of alcohol as shown in Fig. 12. However, the LFP STELLA model cannot be used to predict the superoxide concentration in the continuous photolysis experiment because the time scale is in seconds instead of microseconds. Therefore, a new STELLA model in the time scale of seconds was built, which summarize the LFP model as Eq. (32), showing only the result of triplet branching (See Appendix B for details). Not surprisingly, the expected concentration of superoxide from production increase as alcohol concentration increases as shown in Fig. 13. At higher alcohol concentration, the yield of superoxide is higher.

The superoxide disproportionation is not significant in the LFP STELLA model because the superoxide concentration is small. The continuous photolysis STELLA model accounts for the effect of pH on superoxide decay as shown in Fig. 1 as well as the acceleration due to presence of alcohol. The model, as expected, shows that superoxide concentration is greater in more alkaline conditions, where the superoxide disproportionation rate is small, as shown in Fig. 14. However, the increase in superoxide is limited past pH 13. Once past this pH value, the disproportionation reaction is not

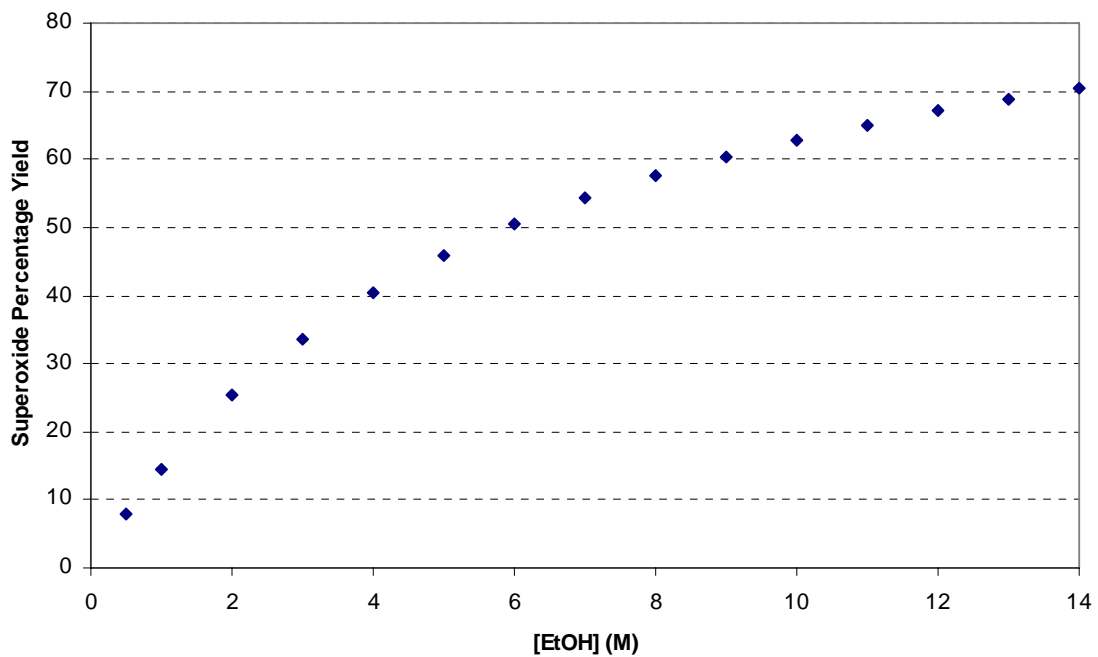


Fig. 12. Superoxide percentage yield as a function of EtOH concentration. The yield is higher as EtOH concentration increases toward absolute ethanol.

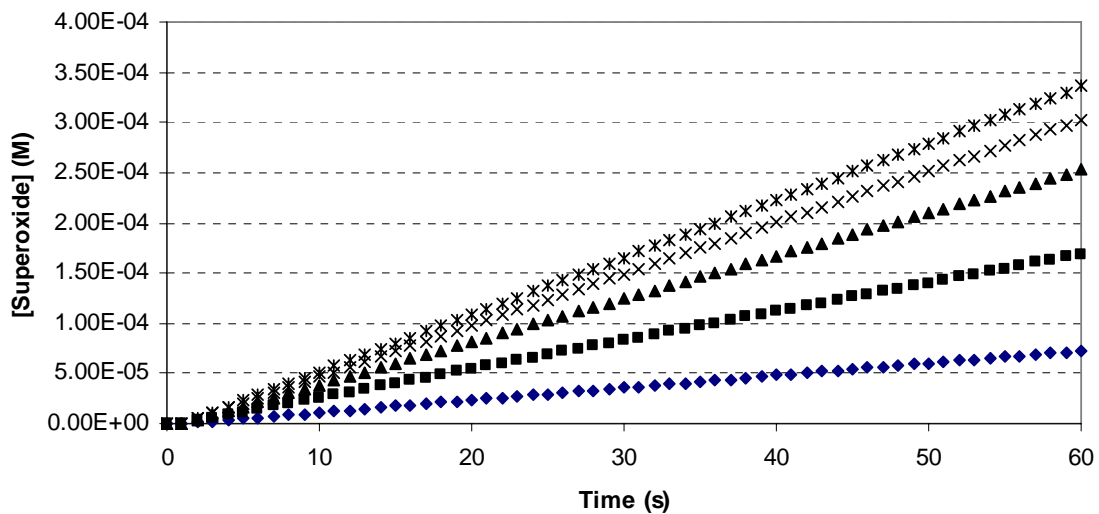


Fig. 13. STELLA simulation of the production of superoxide at various alcohol concentrations at pH 13.5. The diamonds (♦) refer to production at 1 M alcohol, the squares (■) at 3 M, the triangles (▲) at 6 M, the crosses (x) at 9 M, and the asterisks (*) at 12 M. At 12 M, the concentration of superoxide is at highest, indicating that higher alcohol concentration yields more superoxide.

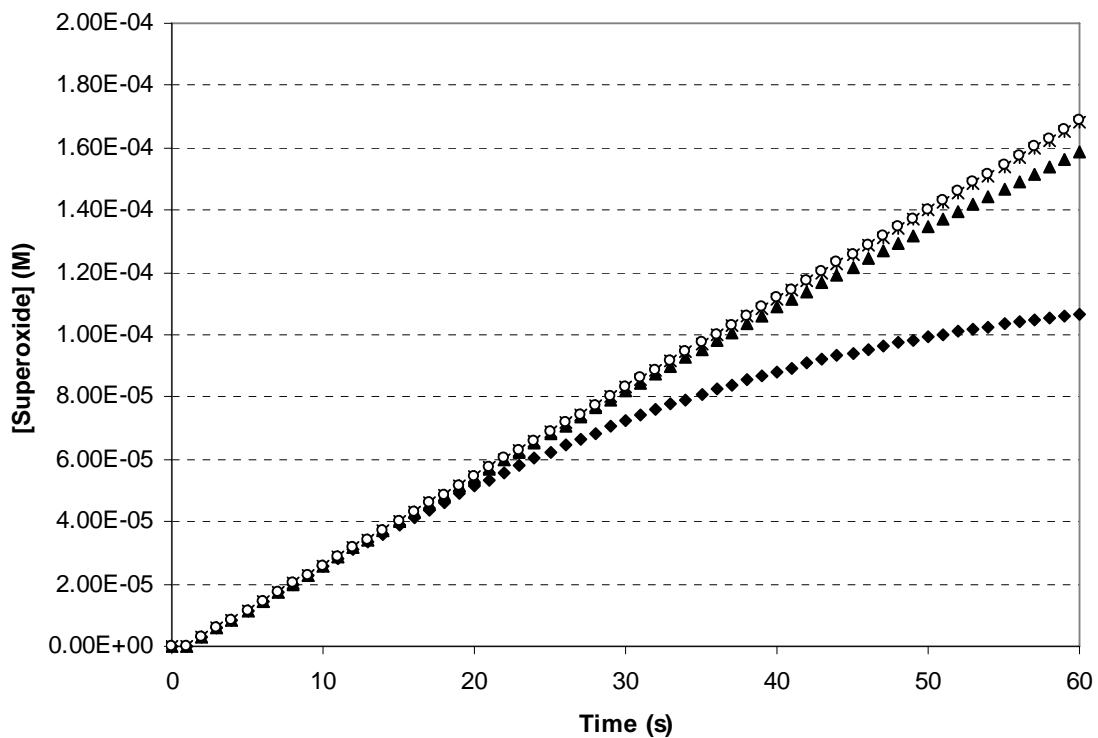


Fig. 14. STELLA simulation of the production of superoxide at various pH in 3 M EtOH. The diamonds (◆) refer to production at pH 11, the triangles (▲) at pH 12, the crosses (x) at pH 13, and the circles (○) at pH 13.5 M. Superoxide produced increases with pH, however, once past pH 13, the production becomes pH independent. The production at pH 13.5 did not increase compared to production at pH 13.

significant compared to the production reaction, and so the superoxide production becomes independent of pH.

From the STELLA simulation, the optimal conditions for superoxide production using the McDowell reaction are at 12-13 M ethanol at pH 13. The result is compared with actual superoxide production photolysis data as shown in Fig. 15 and 16. At constant ethanol concentration (set at 3 M ethanol because before this model was made we were concerned with the effect of alcohol on superoxide decay rate when the continuous photolysis experiments were done) and increasing pH, the theoretical and the experimental values show the same trend of increase but with an error of 50%. However, for constant pH and increasing ethanol concentration, the experiment shows that superoxide production decreases past 9 M, while STELLA predicts a continuous increase. This discrepancy suggests that we do not fully understand the effect of alcohol on the decay rate of superoxide, and that needs to be incorporated in the STELLA model.

As it is, the model requires more work to better predict superoxide concentration produced in the continuous photolysis experiment. More work is needed on the mechanistic information of acetone intermediates, as it is the model uses benzophenone mechanistic information to predict acetone reactions, assuming similarity as according to McDowell et. al. (1983). However, the carbonyl group on the benzophenone is more extensively conjugated than the carbonyl group on the acetone, and this fact may affect the rate information significantly if switching from acetone to benzophenone. The investigation of acetone intermediates by LFP will be difficult because acetone does not absorb well in the 355 nm Nd-YAG laser wavelength. Further second harmonic generation can be used to double the Nd-YAG laser frequency, but the intensity of the

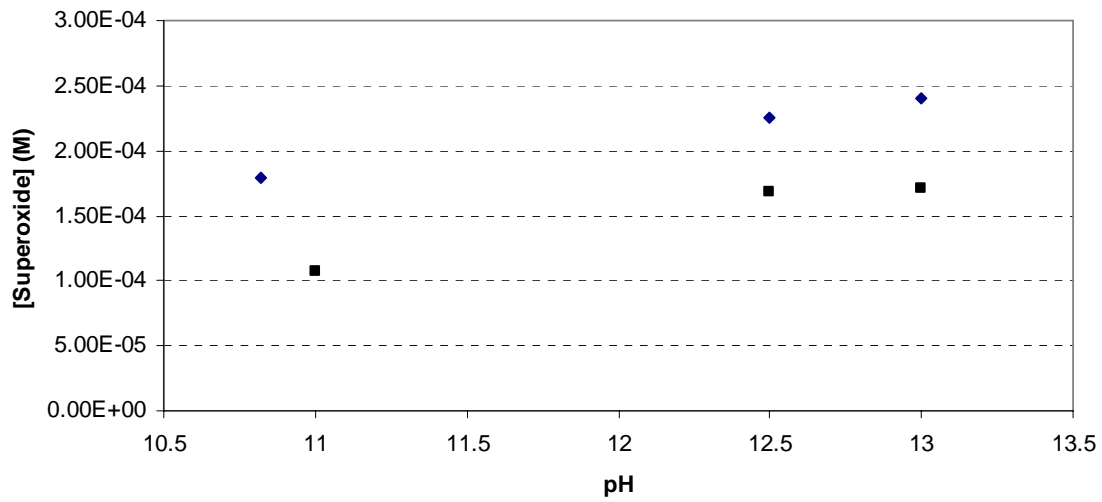


Fig. 15. Superoxide concentration produced as a function of pH at 3 M EtOH. The diamonds (♦) shows the superoxide produced in the actual photolysis experiment, and the squares (■) show the values from STELLA simulation. The results show that the model underestimates the amount of superoxide produced in this condition by 50% but shows the same trend of increase.

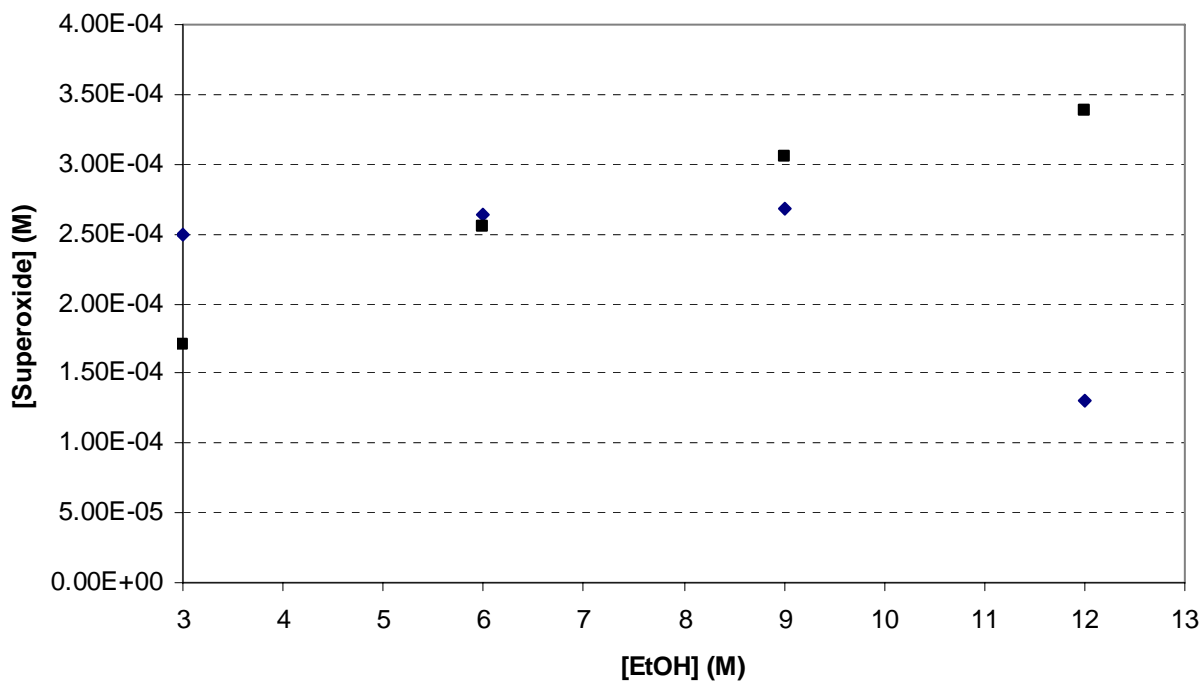


Fig. 16. Superoxide concentration as a function of ethanol concentration at pH 13. The diamonds (♦) show the superoxide produced in the photolysis experiments, and the squares (■) show the values from STELLA simulation. The model and actual photolysis agree with various accuracy, but STELLA predicts the optimal ethanol concentration is at 12 M, while the photolysis shows the optimal concentration at 6-9 M. This discrepancy indicates that the effect of ethanol on superoxide decay is not well captured in the STELLA model.

beam will be much lower. Whether a significant amount of acetone triplets would be produced under this condition needs to be investigated.

Conclusion

This research has investigated the detailed reaction of the photochemical production of superoxide first proposed by McDowell et. al. (1983) by LFP, and a model computational study was done to find the optimal conditions to produce superoxide. The model concludes that the McDowell reaction is best done at 12-13 M ethanol concentration and at pH 13. However, this result is not in agreement with actual photolysis data, which shows that the optimal ethanol concentration is at 9 M. More work is needed to improve the model, including investigation on the effect of alcohol on superoxide decay and investigation on the acetone intermediate mechanism in McDowell reaction.

Future Work

The detail of the effect of alcohol on the rate of superoxide decay should be investigated, and incorporated the result into the model. More continuous photolysis experiments at the optimal conditions specified by the model to gather more data for comparison, specifically experiments with benzophenone and ethanol so conditions would be more similar between the model and the experiment. LFP investigation of acetone triplet reaction with ethanol should be done to observe if the rate information of acetone reaction with ethanol is significantly different than the benzophenone reaction with ethanol.

The continuous photolysis experiment should be used to standardize the MCLA chemiluminescence method which detects superoxide in the micromolar concentration. The micromolar concentration is the natural concentration of superoxide found in natural aquatic media.

Works Cited

- 1) Czapski, G.; Goldstein, S.; Meyerstein, D. *Free Radic. Res. Commun.*, **1988**, 4(4), 231-6.
- 2) Salmon, T. P.; Rose, A. L.; Neilan, B. A.; Waite, T. D. *Limnol. Oceanogr.*, **2006**, 51(4), 1744-54.
- 3) Kustka, A. B.; Shaked, Y.; Milligan, A. J.; King, D. W.; Morel, F. M. M.; *Limnol. Oceanogr.* **2005**, 50(4), 1172-1180.
- 4) Bielski, B. H. J.; Cabelli, D. E.; Arudi, R. L.; *J. Phys. Chem. Ref. Data.* **1985**, 14(4), 1041-1100.
- 5) McDowell, M. S.; Bakac, A.; Espenson, J. H.; *Inorg. Chem.* **1983**, 22, 847-848.
- 6) Fujii, M.; Rose, A. L.; Waite, T. D.; Omuba, T.; *Environ. Sci. Technol.* **2006**, 40, 880-887.
- 7) Shield, S. R.; Harris, J. M.; *Anal. Chem.* **1998**, 70, 2576-2583.
- 8) Canonica, S.; Hellrung, B.; Wirz, J.; *J. Phys. Chem. A* **2000**, 104, 1226-1232.
- 9) Beckett, A.; Porter, G.; *Trans. Faraday Soc.* **1963**, 59(489), 2038-50.

Appendix A – LFP STELLA Model

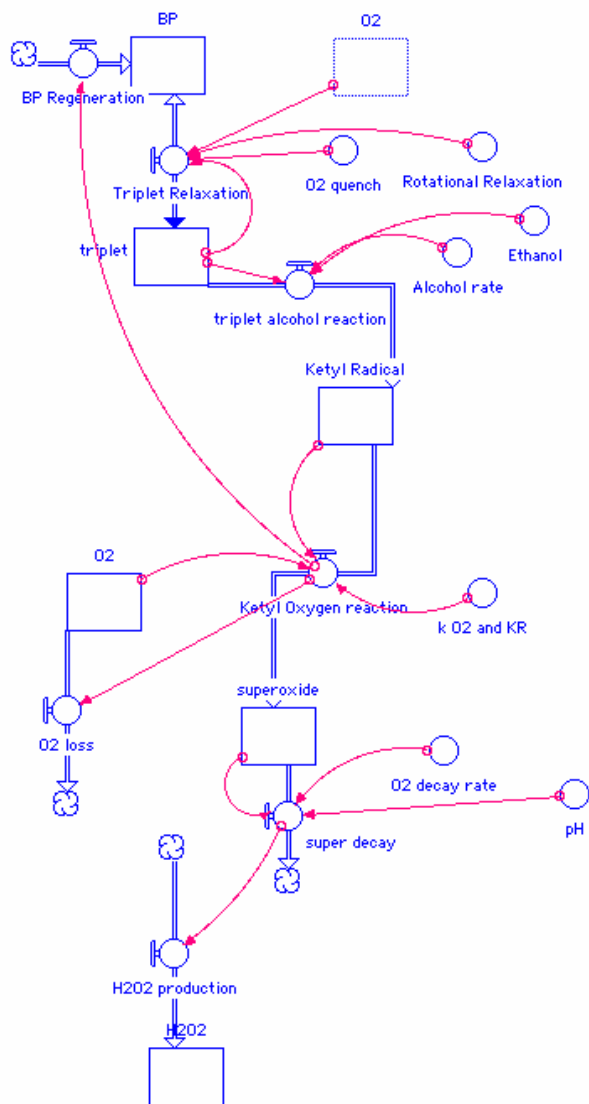


Fig. A1. The LFP STELLA model. The model shows explicitly all the radical intermediate species and is set at a microsecond time scale. The rectangles denote chemical species taking part in the reactions. The “valves” between the rectangles denote intermediate reactions with reaction rate information (reaction rate equations). The circles denote various conditions such as pH, ethanol concentration, etc. The red lines show the dependency of reactions on different conditions.

Reaction Rate Equations of the LFP STELLA model

$BP(t) = BP(t - dt) + (\text{Triplet_Relaxation} + \text{Noname_4}) * dt$
INIT BP = .0025

INFLOWS:

$\text{Triplet_Relaxation} = \text{O2_quench} * \text{O2} * \text{triplet} + \text{triplet} * \text{Rotational_Relaxation}$
 $BP_Regeneration = \text{Ketyl_Oxygen_reaction}$
 $\text{H2O2}(t) = \text{H2O2}(t - dt) + (\text{H2O2_production}) * dt$
INIT H2O2 = 0

INFLOWS:

$\text{H2O2_production} = \text{super_decay} / 2$
 $\text{Ketyl_Radical}(t) = \text{Ketyl_Radical}(t - dt) + (\text{triplet_alcohol_reaction} - \text{Ketyl_Oxygen_reaction}) * dt$
INIT Ketyl_Radical = 0

INFLOWS:

$\text{triplet_alcohol_reaction} = \text{triplet} * \text{Ethanol} * \text{Alcohol_rate}$

OUTFLOWS:

$\text{Ketyl_Oxygen_reaction} = k_O2_and_KR * \text{O2} * \text{Ketyl_Radical}$
 $\text{O2}(t) = \text{O2}(t - dt) + (- \text{O2_loss}) * dt$
INIT O2 = 0.001

OUTFLOWS:

$\text{O2_loss} = \text{Ketyl_Oxygen_reaction}$
 $\text{superoxide}(t) = \text{superoxide}(t - dt) + (\text{Ketyl_Oxygen_reaction} - \text{super_decay}) * dt$
INIT superoxide = 0

INFLOWS:

$\text{Ketyl_Oxygen_reaction} = k_O2_and_KR * \text{O2} * \text{Ketyl_Radical}$

OUTFLOWS:

$\text{super_decay} = 10^{(\text{O2_decay_rate} - \text{pH})} * \text{superoxide} * \text{superoxide}$
 $\text{triplet}(t) = \text{triplet}(t - dt) + (- \text{Triplet_Relaxation} - \text{triplet_alcohol_reaction}) * dt$
INIT triplet = 1e-5

OUTFLOWS:

$\text{Triplet_Relaxation} = \text{O2_quench} * \text{O2} * \text{triplet} + \text{triplet} * \text{Rotational_Relaxation}$
 $\text{triplet_alcohol_reaction} = \text{triplet} * \text{Ethanol} * \text{Alcohol_rate}$
 $\text{Alcohol_rate} = 2.1e6$
 $\text{Ethanol} = 0.5$
 $k_O2_and_KR = 2.3e9$
 $\text{O2_decay_rate} = 13$
 $\text{O2_quench} = 2.6e9$
 $\text{pH} = 11.5$
 $\text{Rotational_Relaxation} = 6.7e5$

Appendix B – The Continuous Photolysis STELLA Model

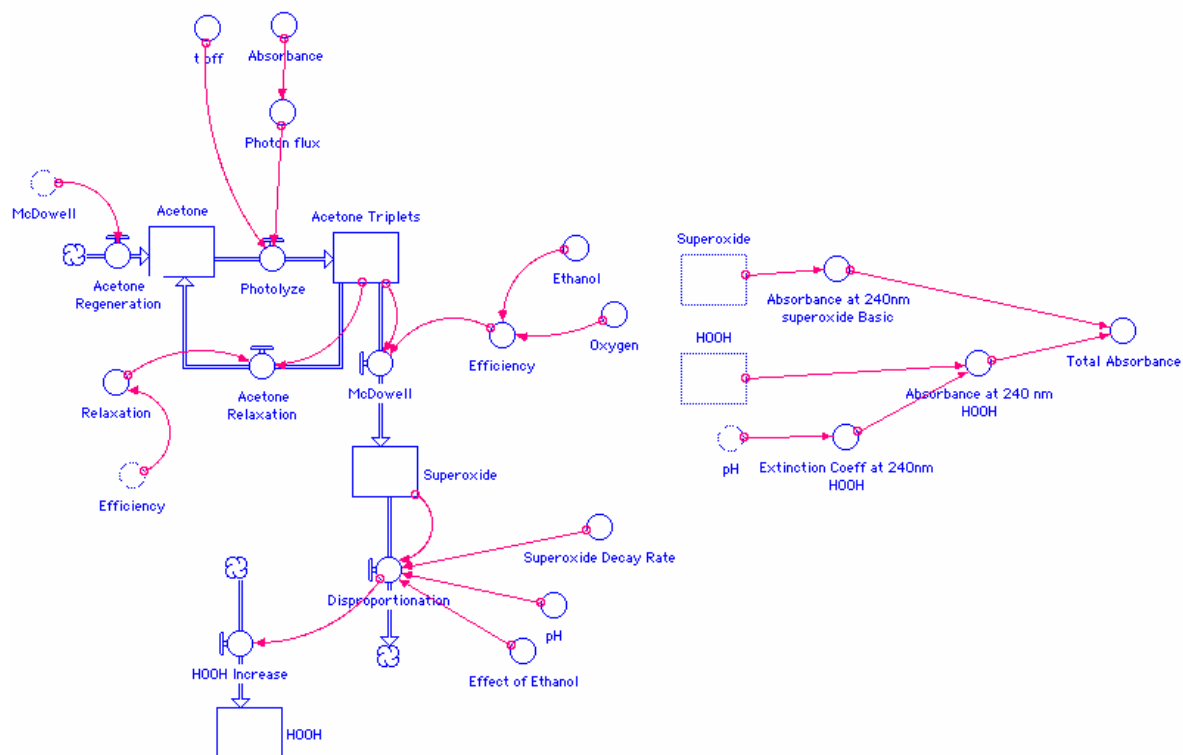


Fig. B1. The continuous photolysis STELLA model. The model does not show explicitly the radical intermediates as the LFP STELLA model. The intermediate reactions are summarized into one reaction “McDowell” using the branching ratio of the triplets as a function of alcohol and oxygen concentration as given by Eq. (32). Also, acetone was used to replace benzophenone to produce ketone triplets, assuming similarity in rate information. The rectangles denote chemical species taking part in the reactions. The “valves” between the rectangles denote intermediate reactions with reaction rate information (reaction rate equations). The circles denote various conditions such as pH, ethanol concentration, etc. The red lines show the dependency of reactions on different conditions.

Reaction Rate Equations of the Continuous Photolysis Stella Model

Acetone(t) = Acetone(t - dt) + (Acetone Relaxation + Acetone Regeneration - Photolyze) * dt
INIT Acetone = 41*10⁻³ M

INFLOWS:

Acetone Relaxation = Relaxation*Acetone Triplets

Acetone Regeneration = McDowell

OUTFLOWS:

Photolyze = IF(TIME<t_off) THEN Photon_flux/0.003 ELSE 0

Acetone_Triplets(t) = Acetone_Triplets(t - dt) + (Photolyze - McDowell - Acetone_Relaxation) * dt

INIT Acetone_Triplets = 0

INFLOWS:

Photolyze = IF(TIME<t_off) THEN Photon_flux/0.003 ELSE 0

OUTFLOWS:

McDowell = Efficiency x Acetone Triplets

Acetone Relaxation = Relaxation*Acetone_Triplets

HOOH(t) = HOOH(t - dt) + (HOOH_Increase) * dt

INIT HOOH = 0

INFLOWS:

HOOH_Increase = 0.5*Disproportionation

Superoxide(t) = Superoxide(t - dt) + (McDowell - Disproportionation) * dt

INIT Superoxide = 0

INFLOWS:

McDowell = Efficiency*Acetone_Triplets

OUTFLOWS:

Disproportionation = Effect_of_Ethanol*10^{^(Superoxide_Decay_Rate-pH)}*Superoxide*Superoxide

Absorbance = 0.5

Absorbance_at_240nm_superoxide_Basic = Superoxide*2345

Absorbance_at_240_nm_HOOH = Extinction_Coeff_at_240nm_HOOH*HOOH

Effect_of_Ethanol = 2

Efficiency = (5.5E5*Ethanol)/(5.5E5*Ethanol+6.7E5+2.6E9*Oxygen)

Ethanol = 13

Extinction_Coeff_at_240nm_HOOH = (10^{^(-11.65)*320})/(10^{^(-11.65)+10^{^(-pH)}})+10^{^(-pH)*31}/(10^{^(-11.65)+10^{^(-pH)}})

Oxygen = 1e-3

pH = 11.5

Photon_flux = 1.5e-7*0.25-(1.5e-7*0.25/10^{^(Absorbance)})

Relaxation = 1-Efficiency

Superoxide_Decay_Rate (Log linearization of the basic portion of the Bielski Curve at pH 0) = 13

Total_Absorbance = Absorbance_at_240nm_superoxide_Basic+Absorbance_at_240_nm_HOOH

t_off = 60